Helicoidal ordering in iron perovskites

Mostovoy, M

Published in:
Physical Review Letters

DOI:
10.1103/PhysRevLett.94.137205

Publication date:
2005

Helicoidal Ordering in Iron Perovskites

Maxim Mostovoy

Max-Planck-Institut für Festkörperforschung, Heisenbergstrasse 1, D-70569 Stuttgart, Germany
Materials Science Center, University of Groningen, Nijenborgh 4, 9747 AG Groningen, The Netherlands

(Received 31 August 2004; published 6 April 2005)

We study the double exchange in transition metal oxides with itinerant and localized electrons. We show that the charge transfer energy Δ and the oxygen-oxygen hopping amplitude t_{pp} have a strong effect on magnetic ordering: while for $\Delta > 0$ the ground state is ferromagnetic, for negative Δ and large t_{pp} the double exchange gives rise to an incommensurate helicoidal ordering of local spins, observed, e.g., in the iron perovskites $SrFeO_3$ and $CaFeO_3$. For negative Δ, the metal-insulator transition into a charge-ordered state has little effect on magnetic ordering. This explains the difference in magnetic and transport properties of ferrates and manganites.

DOI: 10.1103/PhysRevLett.94.137205 PACS numbers: 75.10.–b, 71.30.+h, 75.30.–m, 75.50.Ee

The interaction of itinerant electrons with local spins couples transport to magnetism and gives rise to many fascinating phenomena, e.g., the heavy fermion behavior and colossal magnetoresistance (CMR) effect. Because of the strong Hund's rule coupling between the d electrons in CMR manganites, the hopping amplitudes of the itinerant e_g electrons depend on orientations of spins of the localized t_{2g} electrons, which results in the so-called double exchange (DE) [1–3]. The ground state spin ordering minimizes the kinetic energy of the conduction electrons, and since the width of conduction bands is maximal for parallel spins, it is usually assumed that the DE favors ferromagnetic (FM) state. The DE theory qualitatively explains the ferromagnetism and CMR of doped manganites [4].

However, the DE in transition metal (TM) oxides does not always result in the FM ground state and a strong coupling between transport and magnetism. Thus, the cubic perovskite $SrFeO_3$ below $T_N = 134$ K is a helicoidal magnet with a small wave vector $\mathbf{Q}$ along the body diagonal [5–7]. This material is a metal both above and below the magnetic transition [8] and its resistivity shows no anomaly at T_N [9]. Furthermore, the helicoidal magnetic (HM) ordering with close values of the helix wave vector and Néel temperature ($T_N = 115$ K) is also observed in the charge-ordered insulator $CaFeO_3$ [10,11].

Although the Fe^{4+} ion nominally has the same high-spin d^4 electronic configuration as the Mn^{3+} ion in $LaMnO_3$, the tetravalent ferrates show no orbital ordering, which plays an important role in manganites. This can be explained by the fact that in ferrates the charge transfer energy Δ, i.e., the energy necessary to transfer an electron from an oxygen to a TM ion, is negative: $\Delta \sim -3$ eV [12]. In this case, the conduction bands are formed by the strongly hybridized iron e_g and oxygen p_σ orbitals and a large fraction of charge is carried by the oxygen holes. The electronic configuration of Fe ions is then close to the high-spin d^5 state, which has no orbital degeneracy [12].

In this Letter we show that the magnetic ordering favored by the DE in TM oxides sensitively depends on the charge transfer energy and the oxygen-oxygen hopping amplitude t_{pp}. While for $\Delta > 0$ the ground state is ferromagnetic, for negative Δ and large t_{pp} the double exchange gives rise to an incommensurate HM ordering of local spins. Furthermore, in strongly covalent materials with wide bands, the effect of the transition to a charge-ordered state on magnetic ordering is strongly reduced. This explains the difference in magnetic and transport properties of manganites and ferrates, which is analogous to the difference in orbital and magnetic ordering favored by superexchange interactions in charge transfer and Mott-Hubbard insulators [13,14].

A noncollinear ordering in DE systems is usually explained by the competition between the FM double exchange and antiferromagnetic (AFM) superexchange [3]. However, the states resulting from such a competition are unstable towards phase separation [15] and whether they are observed in doped manganites is still a controversial issue [16]. We show that the HM ordering in ferrates largely results from the DE and that the superexchange plays a minor role here.

The model.—We consider the FM Kondo lattice model, which in addition to itinerant e_g electrons and spins of localized t_{2g} electrons, includes the oxygen p_σ orbitals that are strongly hybridized with the TM e_g orbitals. It is convenient to describe states of the model in terms of holes that can occupy both oxygen and TM sites. By the holes on iron sites we mean the e_g holes in the high-spin electronic d^5 configuration. For infinite Hund's rule coupling, the spin of the e_g hole on the site j is antiparallel to the local spin $\mathbf{S}_j$. The annihilation operator of such a hole is $u_j d_{j\alpha}$, where u_j is the spinor describing the spin-polarized state and the index $\alpha = 1, 2$ denotes, respectively, the $3z^2 - r^2$ and $x^2 - y^2$ orbitals. The holes on oxygen sites can have both spin projections:

$$p_{j\pm b/2} = \begin{pmatrix} p_{j\pm b/2\uparrow} \\ p_{j\pm b/2\downarrow} \end{pmatrix},$$

where $j \pm b/2$ ($b = x, y, z$) are the 6 oxygen sites from the octahedron centered at the TM site j.

The Hamiltonian of the dp model has the form

$$H_{dp} = \sum_{j\alpha b} t_{\alpha b}(d^{\dagger}_{j\alpha} u^{\dagger}_{j} P_{jb} + P^{\dagger}_{jb} u_j d_{j\alpha}) + t_{pp} \sum_{j,b\neq c} P^{\dagger}_{jb} P_{jc} + \Delta \sum_{jb} p^{\dagger}_{j+b/2} p_{j+b/2}, \quad (1)$$

where $P_{jb} = p_{j+b/2} + p_{j-b/2}$. The dp and pp hopping amplitudes are expressed through the Slatter-Koster parameters by $t_1 = (pd\sigma)(-\frac{1}{2}, -\frac{1}{2}, 1)$, $t_2 = (pd\sigma) \times (\frac{\sqrt{3}}{2}, -\frac{\sqrt{3}}{2}, 0)$, and $t_{pp} = \frac{1}{2}(pp\sigma) - \frac{1}{2}(pp\pi)$.

For HM state with the wave vector $\mathbf{Q}$ and spin rotation axis $\mathbf{e_3}$, the local spin on the site j

$$\mathbf{S}_j = S(\mathbf{e}_1 \cos \mathbf{Q}\mathbf{x}_j + \mathbf{e}_2 \sin \mathbf{Q}\mathbf{x}_j), \quad (2)$$

where the unit vectors $\mathbf{e}_1$, $\mathbf{e}_2$, and $\mathbf{e}_3$ form an orthogonal basis. Because of the invariance of the Hamiltonian (1) under an arbitrary rotation of the spin axes, the energy of the HM state is independent of $\mathbf{e}_3$. In $Sr(Ca)FeO_3$, the spin rotation axis is parallel to the helix wave vector [7,11] due to the anisotropy of spin interactions, which we neglect here. For $\mathbf{e}_3 = \hat{x}$ and $\mathbf{e_1} = \hat{z}$, we have

$$u_j = e^{\frac{i}{2}\sigma_x(\mathbf{Q}\mathbf{x}_j)} \begin{pmatrix} 0 \\ 1 \end{pmatrix}.$$

To obtain the hole energies for the HM state, the transformation to the momentum space has to be combined with the spin rotation:

$$p_{j\pm b/2} = \frac{1}{\sqrt{N}} \sum_{\mathbf{k}} e^{i(\mathbf{k} + \frac{1}{2}\sigma_x \mathbf{Q})\mathbf{x}_{j\pm b/2}} p_{\mathbf{k}b},$$

where N is the number of Fe ions. The Hamiltonian (1) then reads

$$H = \sum_{\mathbf{k}\alpha b} t_{\alpha b}(d^{\dagger}_{\mathbf{k}\alpha} P_{\mathbf{k}b\downarrow} + P^{\dagger}_{\mathbf{k}b\downarrow} d_{\mathbf{k}\alpha}) + t_{pp} \sum_{\mathbf{k},b\neq c} P^{\dagger}_{\mathbf{k}b} P_{\mathbf{k}c} + \Delta \sum_{\mathbf{k}b} p^{\dagger}_{\mathbf{k}b} p_{\mathbf{k}b}, \quad (3)$$

where

$$P_{\mathbf{k}b\sigma} = 2\left(\cos\frac{Q_b}{4} \cos\frac{k_b}{2} p_{\mathbf{k}b\sigma} - \sin\frac{Q_b}{4} \sin\frac{k_b}{2} p_{\mathbf{k}b,-\sigma}\right)$$

(the lattice constant equals 1).

The hole bands for the FM state are shown in Fig. 1. For local spins oriented up, the spin-down bands (solid lines) are formed by the mixed d and p hole states, while the spin-up bands (circles) are purely oxygen-hole bands. To a good approximation, the states forming the two lowest bands are Bloch superpositions of the Zhang-Rice states of holes on metal-oxygen octahedra [17] with the symmetry of the $3z^2 - r^2$ and $x^2 - y^2$ orbitals. These are the two bands of the effective dd model used to describe colossal magnetoresistance manganites [15]. Even for ferrates with the almost complete charge transfer from oxygen to iron [18], the Fermi sea is predominantly filled by the states from these two bands (in Fig. 1 the Fermi energy ε_F is indicated by the thin horizontal line).

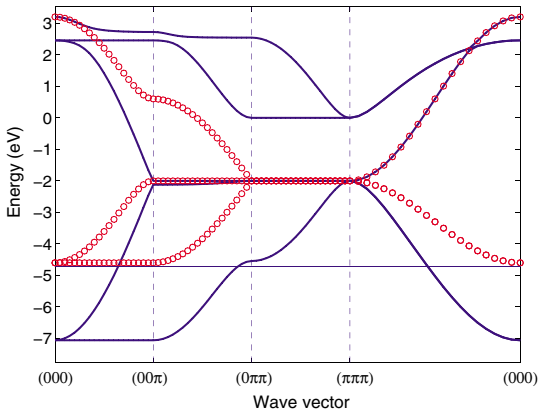

FIG. 1 (color online). The mixed $dp\downarrow$-hole bands (solid lines) and oxygen $p\uparrow$-hole bands (circles) for ferromagnetically ordered local spins, $(pd\sigma) = 1.7$ eV, $t_{pp} = 0.65$ eV, and $\Delta = -2$ eV. The thin horizontal line indicates the Fermi level for $1e_g$ hole/Fe.

Yet for negative Δ, the dd model may fail to describe the magnetic ground state. The reason is the high density of low energy spin-flip excitations, created by promoting a hole from the spin-down Fermi sea to one of the two lowest oxygen spin-up bands, which can make the FM state unstable towards the HM spin ordering. In the HM state these bands become mixed with the two lowest dp bands, which lowers the energies of the occupied states. There is also an energy loss due to the narrowing of bands caused by the relative rotation of local spins (the usual DE mechanism). When the bottom of the oxygen spin-up bands (at $\varepsilon = \Delta - 4t_{pp}$) is close to ε_F, the energy gain exceeds the energy loss, which stabilizes the HM state.

The FM-HM transition, similar to the spin-density-wave (SDW) instability, is driven by the lowering of the energy of occupied states. However, it does not require a nested Fermi surface and does not open a gap, since the crossing of the spin-up and spin-down bands only occurs at isolated points of the Fermi surface. While at SDW transitions the energy is gained close to ε_F, in our case the energy gain is distributed over the whole Fermi sea—it is a Fermi sea rather than a Fermi surface instability.

The transition from the FM to HM ground state, induced by varying Δ, $(pd\sigma)$, and t_{pp}, is shown Fig. 2, where we plot the optimal angle ϕ between the spins in neighboring [100] layers [$\mathbf{Q} = \phi(1, 0, 0)$ and $\phi = 0$ corresponds to the FM state]. In general, the helical angle ϕ grows with the weight of oxygen holes in the ground state, which can be achieved by decreasing Δ or the width of the dp bands [see Figs. 2(a) and 2(b)], or by increasing the width of the oxygen bands [see Fig. 2(c)]. To a good approximation,

the value of ϕ is controlled by a single parameter $\delta = (\varepsilon_F - \Delta + t_{pp})/(pd\sigma)$, describing the separation between the Fermi energy and the bottom of the oxygen spin-up band in the FM state. When the data shown in Figs. 2(a)–2(c) are replotted versus δ, they nearly fall on a single curve [see Fig. 2(d)]. The FM state becomes unstable for small negative δ, when the bottom of the oxygen band is slightly above the Fermi energy. The change of the magnetic ordering from HM to FM upon applied pressure, which widens conduction bands, was reported in Ref. [19].

Effect of superexchange.—The double exchange by itself favors the HM state with $\mathbf{Q}$ parallel to one of the cubic axes (A-type HM state), while in $SrFeO_3$ the helix is parallel to the body diagonal (G-type HM state). The dependence of the energy on the direction of $\mathbf{Q}$ is, however, very weak: the energy increases by ~ 10 K/Fe, when $\hat{\mathbf{Q}} = \frac{\mathbf{Q}}{Q}$ varies from $(1, 0, 0)$ to $\frac{1}{\sqrt{3}}(1, 1, 1)$. Therefore, $\hat{\mathbf{Q}}$ can be affected by relatively weak interactions, of which the most important is the AFM superexchange (SE) between the local spins,

$$H_{\mathrm{SE}} = J\sum_{ib}(\mathbf{S}_i\mathbf{S}_{i+b}), \qquad J > 0. \tag{4}$$

In Fig. 3(a) we plot the phase diagram of the DE model Eq. (1). As Δ decreases, the FM state undergoes a second-order transition to the A-type HM state. The critical value of the charge transfer energy grows with increasing t_{pp} and eventually becomes positive. Thus a large oxygen-oxygen hopping amplitude is also important for stabilization of the HM state. The effect of the weak SE interaction $\frac{J}{(pd\sigma)} = 0.002$ is shown in Fig. 3(b). The region occupied by the A-type HM state shrinks. As Δ decreases, this state is replaced by the A-type AFM state, which then undergoes a first-order transition to the incommensurate G-type HM state, favored by the SE interaction. The SE interaction also stabilizes the G-type HM state at very large positive Δ, when holes predominantly occupy TM sites and the effective dd hoping $\sim \frac{(pd\sigma)^2}{\Delta}$ is small, so that kinetic and SE energies are comparable [3].

Helicoidal ordering in insulators.—Since the instability of the FM state towards a HM ordering is a Fermi sea rather than a Fermi surface instability, it can also occur in insulators, such as $CaFeO_3$ below the charge ordering temperature $T_{\mathrm{CO}} = 290$ K. We assume that the driving force of this charge ordering is the electron-lattice coupling, which results in the breathing-type lattice distortion (an alternation of large and small oxygen octahedra) below T_{CO} [11]. Figure 4 shows the dependence of the gap in the hole spectrum (squares) due to the modulation of the hopping amplitudes in the ordered state: $t_{\alpha b}(i) = (1 + \sigma_i\eta)t_{\alpha b}$ and $t_{pp}(i) = (1 + \sigma_i\eta)t_{pp}$, where $\sigma_i = \pm 1$ for $i \in A/B$ sublattice of the cubic lattice. Since the Fermi surface is not nested, the gap only opens above some critical value of the modulation amplitude η. The helical angle ϕ (circles) decreases very slowly with η and even the 1 eV gap has little effect on the helical wave vector.

Magnon dispersion.—The magnon spectrum for the A-type HM state, calculated in the leading $1/S$ approximation, is shown in Fig. 5 (details of this calculation will

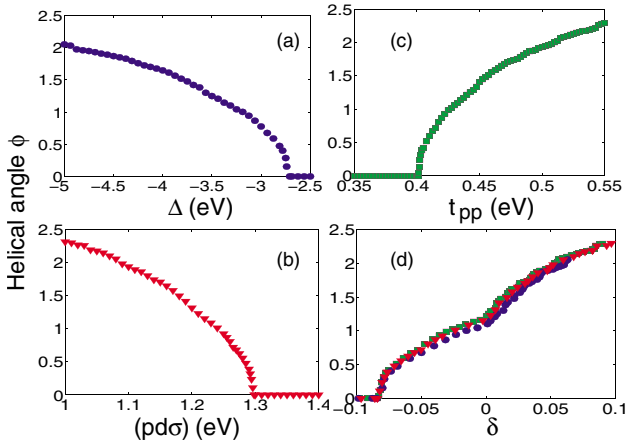

FIG. 2 (color online). The helical angle ϕ (in radians) between the spins in neighboring [100] layers plotted vs: (a) Δ, for $(pd\sigma) = 1.3$ eV and $t_{pp} = 0.4$ eV; (b) $(pd\sigma)$, for $\Delta = -2.7$ eV and $t_{pp} = 0.4$ eV; (c) t_{pp}, for $(pd\sigma) = 1.3$ eV and $\Delta = -2.7$ eV. These three curves are replotted vs $\delta = (\varepsilon_F - \Delta + 4t_{pp})/(pd\sigma)$ in the panel (d).

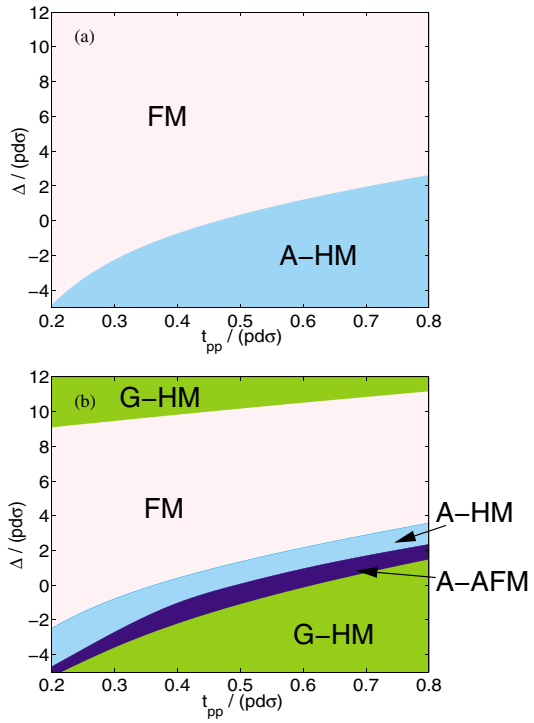

FIG. 3 (color online). The phase diagram of the dp model (1) [panel (a)] and the dp model plus the SE interaction $\frac{J}{(pd\sigma)} = 0.002$ [panel (b)]. Here A-HM and G-HM denotes the HM state with, respectively, $\mathbf{Q} = \phi(1, 0, 0)$ and $\mathbf{Q} = \phi(1, 1, 1)$, while A-AFM denotes the A-type AFM state with $\mathbf{Q} = \pi(1, 0, 0)$.

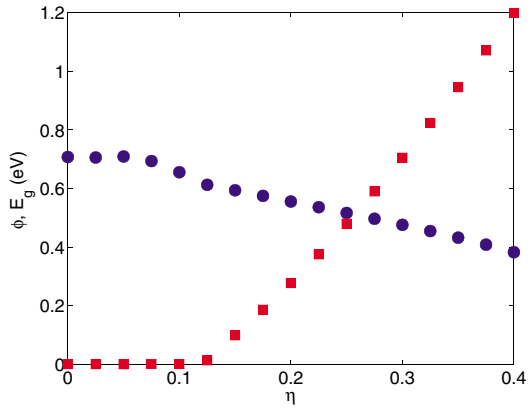

FIG. 4 (color online). The helical angle ϕ between the [111] layers (circles), measured in radians, and the gap E_g (squares), measured in eV, vs the modulation amplitude η for $(pd\sigma) = 1.7$ eV, $t_{pp} = 0.65$ eV, and $\Delta = -3$ eV.

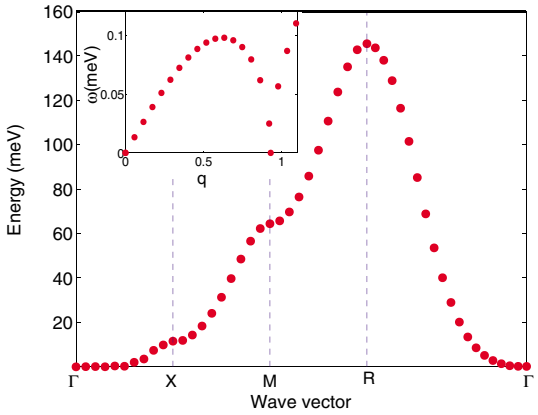

FIG. 5 (color online). The magnon spectrum for the helicoidal state with $\mathbf{Q} = 0.93(1, 0, 0)$, which is the ground state for $(pd\sigma) = 1.7$ eV, $t_{pp} = 0.65$ eV, and $\Delta = -2$ eV. The inset shows $\omega_{\mathbf{q}}$ for $\mathbf{q} = q(1, 0, 0)$, where q varies between 0 and $1.2Q$.

be published elsewhere). The magnon frequency vanishes both at $\mathbf{q} = 0$ and $\mathbf{q} = \mathbf{Q}$, corresponding to the two Goldstone modes: the translation of the incommensurate helix along $\mathbf{Q}$ and rotation of the helical axis $\mathbf{e}_3$, respectively. Although the HM state is stable, the magnon spectrum for $\mathbf{q}$ varying between 0 and $\mathbf{Q}$ is extremely soft (note the small energy scale in the inset in Fig. 5).

At the transition from HM to FM state, these two points merge, resulting in the vanishing spin stiffness. Thus the transition from HM to FM state at zero temperature, which can be induced by varying Δ, $(pd\sigma)$, or t_{pp} (see Fig. 2), is a quantum critical point, at which both the Curie and Néel temperatures drop to zero due to diverging spin fluctuations. In reality, such a quantum critical behavior is suppressed by the single-ion and exchange anisotropies, neglected in our model, which open a gap in the magnon spectrum at $\mathbf{q} = \mathbf{Q}$ and result in a first-order transition between the two magnetic states. This may explain why the magnetic ordering temperature in $SrFeO_3$ seems to monotonously grow with pressure when the HM state is replaced by the FM state [19].

In conclusion, the double exchange does not always favor ferromagnetism. The kinetic energy of conduction electrons strongly coupled to local spins can be minimized by the helicoidal spin ordering. The smaller width of the conduction bands in the helicoidal state is compensated by the higher density of states. This explains the incommensurate helicoidal ordering observed in the negative charge transfer energy materials, $SrFeO_3$ and $CaFeO_3$. The antiferromagnetic superexchange plays here a relatively minor role. The transition to a charge-ordered state does not strongly affect the magnetic ordering, in agreement with the decoupling of transport and magnetism observed in ferrates. Thus, the behavior of transition metal oxides close to the metal-insulator transition sensitively depends on the value of the charge transfer energy.

I would like to thank B. Keimer, G. Khaliullin, D. Khomskii, O. Sushkov, B. Simons, and C. Ulrich for fruitful discussions.

[1] C. Zener, Phys. Rev. **81**, 440 (1951); **82**, 403 (1951).
[2] P. W. Anderson and H. Hasegawa, Phys. Rev. **100**, 675 (1955).
[3] P.-G. de Gennes, Phys. Rev. **118**, 141 (1960).
[4] *Colossal Magnetoresistive Manganites*, edited by Y. Tokura (Gordon and Breach, New York, 2000).
[5] M. Takano *et al.*, Mater. Res. Bull. **12**, 923 (1977).
[6] T. Takeda, Y. Yamaguchi, and H. Watanabe, J. Phys. Soc. Jpn. **33**, 967 (1972).
[7] H. Oda, Y. Yamaguchi, H. Takei, and H. Watanabe, J. Phys. Soc. Jpn. **42**, 101 (1977).
[8] J. B. MacChesney *et al.*, J. Chem. Phys. **43**, 1907 (1965).
[9] A. Lebon *et al.*, Phys. Rev. Lett. **92**, 037202 (2004).
[10] S. Kawasaki, M. Takano, R. Kanno, T. Takeda, and A. Fujumori, J. Phys. Soc. Jpn. **67**, 1529 (1998).
[11] P. M. Woodward *et al.* Phys. Rev. B **62**, 844 (2000).
[12] A. E. Bocquet *et al.*, Phys. Rev. B **46**, 3771 (1992).
[13] J. Zaanen, G. A. Sawatzky, and J. W. Allen, Phys. Rev. Lett. **55**, 418 (1985); J. Zaanen and G. A. Sawatzky, Can. J. Phys. **65**, 1262 (1987).
[14] M. V. Mostovoy and D. I. Khomskii, Phys. Rev. Lett. **89**, 227203 (2002); **92**, 167201 (2004).
[15] See, e.g., E. Dagotto *et al.*, Phys. Rep. **344**, 1 (2001).
[16] J. Geck *et al.*, Phys. Rev. B, **64**, 144430 (2001) and references therein.
[17] F. C. Zhang and T. M. Rice, Phys. Rev. B **37**, 3759 (1988).
[18] For the set of parameters for $SrFeO_3$: $(pd\sigma) = 1.3$ eV, $t_{pp} = 0.4$ eV, and $\Delta = -3$ eV [12]; the weight of the iron d^5, d^4, and d^3 configurations is, respectively, 0.81, 0.18, and 0.01.
[19] S. Nasu, T. Kawakami, S. Kawasaki, and M. Takano, Hyperfine Interact. **144/145**, 119 (2002).